Mosquito and primate ecology predict human risk of yellow fever virus spillover in Brazil

Marissa L. Childs[1*], Nicole Nova[2], Justine Colvin[2], Erin A. Mordecai[2]

[1]Emmett Interdisciplinary Program in Environment and Resources, Stanford University, Stanford, CA 94305, USA
[2]Biology Department, Stanford University, Stanford, CA 94305, USA
[*]To whom correspondence should be addressed: marissac@stanford.edu, ORCID ID 0000-0002-8597-2161

Keywords: yellow fever, pathogen spillover, disease ecology, Brazil, vector-borne disease, mosquito

Abstract
Many (re)emerging infectious diseases in humans arise from pathogen spillover from wildlife or livestock, and accurately predicting pathogen spillover is an important public health goal. In the Americas, yellow fever in humans primarily occurs following spillover from non-human primates via mosquitoes. Predicting yellow fever spillover can improve public health responses through vector control and mass vaccination. Here, we develop and test a mechanistic model of pathogen spillover to predict human risk for yellow fever in Brazil. Our environmental risk model, based on the ecology of mosquito vectors and non-human primate hosts, distinguished municipality-months with yellow fever spillover from 2001 to 2016 with high accuracy (AUC = 0.71). Incorporating hypothesized cyclical dynamics of infected primates improved accuracy (AUC = 0.79). Using boosted regression trees to identify gaps in the mechanistic model, we found that important predictors include current and lagged (mechanistic) environmental risk, vaccine coverage, population density, temperature, and precipitation. More broadly, we show that for a widespread human viral pathogen, the ecological interactions between environment, vectors, reservoir hosts, and humans can predict spillover with surprising accuracy, suggesting the potential to improve preventative action to reduce yellow fever spillover and prevent onward epidemics in humans.

Introduction

Many important (re)emerging infectious diseases in humans—including Ebola, sudden acute respiratory syndrome (SARS), influenza, *Plasmodium knowlesi* and other primate malarias, yellow fever, and leptospirosis—arise from spillover of pathogens from wildlife or livestock into human populations (1,2). While spillover is an important mechanism of human disease emergence, the drivers and dynamics of spillover are poorly understood and difficult to predict (3). Pathogen spillover requires favorable conditions to align in the reservoir (non-human animal), human, and pathogen populations and in the environment (3–5). Because these conditions interact, nonlinear relationships among the environment, host populations, and spillover probability are likely to emerge. Moreover, spillover is a probabilistic process that does not always occur, even when suitable conditions align. Despite these challenges, it is critical to predict pathogen spillover to enhance public health preparedness. Predicting spillover also provides an opportunity to test ecological approaches to solving globally important human health problems.

Most previous attempts to predict pathogen spillover have used statistical models (6–8). These models may be locally accurate for within-sample prediction, but may struggle to detect multidimensional, nonlinear, and stochastic relationships among host populations, pathogens, the environment, and spillover. In contrast, mechanistic models can test our understanding of transmission ecology, reproduce the complex, nonlinear interactions emerging in disease systems, and potentially improve our ability to predict spillover. In particular, Plowright et al. (3) recently proposed a mechanistic model, which remains untested, that integrates multiple ecological requirements to predict when conditions will align for pathogen spillover. Yellow fever in Brazil presents an ideal opportunity to test this model because the ecology of the pathogen has been studied for nearly 120 years (9), providing a wealth of mechanistic information and data, and because almost all recent cases in South America have occurred via spillover from the sylvatic cycle (10,11)

Yellow fever virus is a mosquito-borne *Flavivirus* that mainly persists in a sylvatic transmission cycle between forest mosquitoes (primarily *Haemagogus janthinomys, Hg. leucocelaenus,* and *Sabethes chloropterus* in South America) and non-human primates, and occasionally spills over into human populations (12). In some settings, these spillover events lead to onward human epidemics in an urban transmission cycle between humans and *Aedes aegypti* mosquitoes (9). Spillover of yellow fever requires the virus to be transmitted locally, mosquito vectors to acquire the virus from infected non-human vertebrate hosts, survive the extrinsic incubation period, and feed on human hosts, and human hosts to be susceptible to infection following exposure. These events require distributions of reservoirs, vectors, and humans, their interactions, and immune dynamics to align in space and time. In humans, yellow fever is the most severe vector-borne virus circulating in the Americas (10) with an estimated fatality rate for severe cases of 47% (13). While no urban transmission of yellow fever has occurred in the Americas since 1997 (14) and in Brazil since 1942 (15), a large epidemic began in December 2016 in Minas Gerais and by June 2018 had caused 2,154 confirmed cases and 745 deaths (16). Despite these large case numbers, molecular and epidemiological evidence suggests that human cases were caused by spillover from the sylvatic cycle, rather than urban transmission (11), most recently in areas previously believed to be free of yellow fever.

Prior statistical models have found climate and weather (including precipitation, temperature, and normalized difference vegetation index), non-human primate richness, land use intensiveness, and a latitudinal gradient to be predictive of the spatial and spatio-temporal distribution of yellow fever (6,8). Here, we build on previous efforts by incorporating a mechanistic understanding of how ecological and human population factors affect yellow fever

transmission and spillover. A mechanistic model allows for known relationships between the environment and transmission mechanisms, estimated from empirical data, to be included to test our understanding of the disease ecology. Additionally, mechanistic models allow for extrapolation beyond known regions to predict other regions where conditions are also suitable for yellow fever spillover. We use a mechanistic model encapsulating sylvatic yellow fever ecology to predict the spatial and temporal distribution of yellow fever spillover in Brazil, and we test the model on human yellow fever case data using a receiver operating characteristic curve and logistic regression. We then extend the statistical analyses in a boosted regression tree analysis to understand what mechanisms our model does not capture. Specifically, we ask: (1) Does the environmental suitability for sylvatic vectors, reservoir hosts, vector-human contact, and mosquito transmission—together termed environmental risk—predict geographic, seasonal, and interannual variation in yellow fever virus spillover into humans? (2) Are human population size and vaccine coverage, above and beyond environmental risk, critical for predicting spillover? (3) What additional environmental and population drivers might improve predictions of spillover? (4) Do the ecological processes that predict spillover in other parts of Brazil predict the recent yellow fever outbreak in the Southeast region of Brazil in 2016–2018, and if so, was risk elevated above historical baseline levels?

Methods

Spillover model

Yellow fever spillover risk is estimated monthly from January 2001 to June 2018 using an adapted version of the model from Plowright et al. (3). We define environmental risk at a location $\vec{y}$ and time t —proportional to the number of infectious mosquito bites—as:

$$b(\vec{y},t)\beta_h(\vec{y},t)\int_{\tau=0}^{\tau=t}\int_{\vec{x}}\rho_h(\vec{x},\tau)b(\vec{x},\tau)\beta_p(\vec{x},\tau)\kappa(\vec{x},\tau)EIP(T(\vec{x},\tau),t-\tau)s(T(\vec{x},\tau),t-\tau)d(\|\vec{y}-\vec{x}\|)dxd\tau \quad (1)$$

as a function of primate range (Fig. 1a), sylvatic mosquito density (Fig. 1b and 1h), probability of biting humans versus non-human primates (Fig. 1c and 1f, respectively), non-human primate infection prevalence, and mosquito biting rate, probability of becoming infectious (Fig. 1g), survival (Fig. 1e), and dispersal (Fig. 1d), as defined in Table 1. We define four metrics of model-predicted yellow fever spillover risk. First, we approximate *environmental risk* (Eq. 1), assuming that biting rate and reservoir infection prevalence are constant over space and time in the absence of empirical data on these parameters, as described in Table 1. Second, we define *immunological-environmental risk* as environmental risk multiplied by the estimated proportion of the human population that is susceptible to yellow fever, using previously estimated vaccine coverage rates (17). Third, we define *population-scaled risk* as the immunological-environmental risk scaled by the number of people in a given location. Fourth, *periodic-environmental risk* uses a phenomenological periodic curve designed to represent cycles of reservoir infection prevalence, driven by the demography of primate populations as naïve individuals are born, susceptible individuals accumulate, and epizootics become more likely (18). Given limited information on the vector species, we use data for *Hg. janthinomys, Hg. leucocelaenus,* and *Sa. chloropterus* to fit models for the sylvatic vectors collectively for all mechanistic vector trait models. We fit each of these parameters as a spatially- and temporally-explicit probability distribution using empirical data, as described below. All data used were publicly available or results from previously published papers, as described in the Supplementary Materials (Table S1 and Mechanistic sub-model details). The full spillover model was run in Google Earth Engine (19).

Mechanistic sub-models

Additional details on mechanistic model methods and data are available in the Supplementary Materials. For primate distribution, human susceptibility, and human population density, we used previously published estimates (17,20,21). All other mechanistic models (terms in Eq. 1) were fit with the R programming language, version 3.5.1 (22), with additional packages used for data processing, manipulation, and visualization (23–31).

Mosquito distribution and seasonal density

To estimate the geographic distribution of sylvatic vector species (Fig. 1b), we fit a species distribution model (32,33) to *Hg. janthinomys, Hg. leucocleanus,* and *Sa. chloropterus* occurrence data identified from the Global Biodiversity Information Facility (GBIF) and a review of the literature, using the maxnet package in R (34). We included maximum, median, and minimum annual land surface temperature, total annual precipitation, precipitation in the driest month, precipitation in the wettest month, elevation, forest cover (%), land cover category, median annual enhanced vegetation index, and absolute latitude as predictors in the model (Supplementary Materials, Table S2). To account for uneven sampling effort across the geographic range, we corrected the background (pseudo-absence) points by subsampling from occurrence data of other mosquito species from GBIF. We calculated mosquito density as $\log\left(\frac{1}{1-p}\right)$, where p is the probability of occurrence estimated from the species distribution model (35). To estimate seasonal variation in vector abundance (Fig. 1h) due to rainfall seasonality (36), we fit a logistic regression of relative monthly mosquito abundance on current and lagged relative monthly rainfall using field data (37–42) with glm in R.

Mosquito survival

To capture effects of temperature on mosquito survival (Fig. 1e), we used empirical data (43–45) and Bayesian inference to fit a quadratic function to the relationship between lifespan and temperature using rstan in R (46). Assuming constant mosquito mortality at a given temperature, we calculated daily survival probability as $p = e^{-1/L}$, where L is mosquito lifespan (47).

Mosquito infectiousness

Virus infection, dissemination, and infectiousness in the mosquito are temperature-dependent (Fig. 1g) (48). We assume that vector competence—the probability that a mosquito exposed to an infectious blood meal becomes infectious with virus in its salivary glands—is a quadratic function of temperature, as shown for other flaviviruses (49). Additionally, we assume that at a given temperature, the extrinsic incubation period—the length of time required for an exposed vector to become infectious—is log-normally distributed across individuals (50,51). We fit a Bayesian model using experimental data (52–59) with the package rstan (46).

Mosquito dispersal

To estimate the range on which sylvatic mosquitoes disperse (Fig. 1d), we fit a negative binomial dispersal kernel (60) to mark-recapture data (61) using a Bayesian framework with the package rstan (46).

Phenomenological primate dynamics

Primate population dynamics and susceptibility have been suggested as important constraints on yellow fever spillover (18), which remain poorly characterized. Assuming that human spillover events are a proxy for infection prevalence during reservoir epizootics, we fit a

phenomenological sine curve with a seven year period (62) to the yearly number of municipality-months with spillover (Fig. 1j) and then transformed the curve to be positive and less than one (Supplementary Materials, Fig. S7). The resulting curve is used as a spatially constant estimate of primate reservoir infection prevalence. We do not scale the curve to any estimate of maximum reservoir infection prevalence as any scaling will only scale the entire risk metric. Phenomenological primate dynamics are used in the periodic-environmental risk estimate to account for a missing ecological process but are not used in any other risk metric, so all other risk metrics are parameterized independent of human spillover data.

Model-data comparison

We compared spatially- and temporally-explicit mechanistic model predictions for spillover risk to observed human cases of yellow fever spillover using a statistical model. We considered four modeled risk metrics (defined above): environmental risk, immunological-environmental risk, population-scaled risk, and periodic-environmental risk. Because municipalities contain heterogeneous environments, we considered both mean risk and maximum risk in each municipality and month, to determine which better captured patterns in the observed spillover data. For each modeled risk metric and each municipality summary statistic (mean and maximum), we fit a logistic regression of spillover probability as a function of model-predicted risk (Supplementary Materials, Table S4) using glm in R (22). Additionally, we calculated a receiver operating characteristic curve to calculate the area under the curve (AUC) for each model, a measure of goodness of fit. We also regressed the number of reported yellow fever cases given that spillover occurred on all eight mechanistic predictions and estimated vaccine coverage (Supplementary Materials, Table S5).

Boosted regression tree

To understand how the mechanistic model could be improved, we used a boosted regression tree (63,64) with current and lagged maximum predicted environmental risk, current and lagged fire area, average and maximum number of primate species, estimated vaccine coverage, human population density, average monthly air temperature, monthly precipitation, phenomenological primate dynamics, region, and month to predict yellow fever spillover for every municipality-month observation (Supplementary Materials, Table S6; 6,8). While some of these covariates are included in the environmental risk metric (i.e., air temperature, rainfall, and primate reservoir ranges), we also include them in the boosted regression tree analysis to identify whether the environmental covariates have any predictive power beyond their role in the mechanistic model, which would indicate that the mechanistic model does not fully capture their influence on spillover. We include fire area as a proxy for land conversion (65), which has previously been shown to be predictive of yellow fever spillover (8). We also include vaccine coverage and human population density despite their poor predictive performance in the mechanistic model to identify whether these human population factors are predictive of spillover in ways not previously hypothesized, and therefore not captured in the mechanistic model. Boosted regression trees repeatedly fit regression trees, which create multiple binary splits in the dataset based on predictor variables. Each successive tree is fit to the residuals of the previous best model. The model is then updated to include the next tree (63). Variable importance is calculated as a weighted sum of the number of times a variable is used for splitting, with weights determined by the squared improvement due to the split (63).

We partition the dataset into training (80%) and test (20%) sets prior to the analysis. Optimal learning rate, tree complexity, and number of trees were selected as the set of parameters that minimized cross-validation predictive deviance (Supplementary Materials,

Table S7; 63). Models were fit in R using the gbm and dismo (66,67) packages, and variable effects were calculated with the pdp package (68). Additional details can be found in the Supplementary Materials.

Results

Primate species distribution (Fig. 1a), vector distribution (Fig. 1b; Supplementary Materials, Fig. S1 and S2), reservoir-vector contact (Fig. 1c), human-vector contact (Fig. 1f), and human susceptibility (Fig. 1i) vary over space and time based on estimates and models fit to empirical data. In addition, vector survival (Fig. 1e) and infectiousness (Fig. 1g, Supplementary Materials, Fig. S4 and S5) vary with temperature, mosquito abundance varies seasonally with rainfall (Fig. 1h; Supplementary Materials, Fig. S3 and Table S3), and mosquito dispersal declines exponentially with distance (Fig. 1d; Supplementary Materials, Fig. S6). Together, these empirical relationships between environment and host, vector, and virus ecology compose an estimate of environmental risk of yellow fever spillover.

The environmental risk model strongly predicted episodes of yellow fever spillover into humans (AUC = 0.71) and adding phenomenological periodic reservoir infection dynamics further improved the model (AUC = 0.79; Fig. 2). Surprisingly, models that included human vaccination coverage and human population size performed worse than the environment-driven models (AUC = 0.63 and 0.61, respectively; Fig. 2). For all risk metrics, maximum value in the municipality-month was a better predictor of spillover than mean value (Fig. 2). Logistic regressions of spillover probability as a function of model-predicted risk showed similar patterns in Akaike Information Criterion (AIC) values (Supplementary Materials, Table S4). All model-predicted risk metrics except mean population-scaled risk were statistically significant predictors of spillover probability at the 5% level. By contrast, given that spillover occurred, none of the eight mechanistic model risk summaries were statistically significant (at 5% level) predictors of number of cases, but vaccine coverage was a statistically significant negative predictor of number of cases ($p = 0.032$; Supplementary Materials, Table S5). This suggests that environmental risk governs the occurrence of spillover while population vaccination can limit the extent of spillover under environmentally favorable conditions.

Mechanistic model estimates closely matched seasonal variation in spillover, and accurately captured differences in seasonality by region (Fig. 3). Risk peaks in April in the North and Northeast regions and in February in Central-West, South, and Southeast regions. The seasonal regional correlation between number of municipality-months with spillover and average environmental risk was highest in the Southeast (0.77), followed by the South (0.61), Central West (0.58), and North (0.42) regions. The periodic-environmental risk matched interannual variation in spillover (Fig. 3); interannual regional correlations were weaker than seasonal correlations but similarly highest in the Southeast (0.55), followed by the Central-West (0.45), North (0.21), and South (0.13) regions.

The boosted regression tree significantly improved predictive performance from the mechanistic model (training AUC > 0.99, test AUC = 0.95) and found lagged environmental risk and current environmental risk to be the first and fourth most important predictors of spillover, respectively (Fig. 4). Vaccine coverage, temperature, population density and precipitation were also among the six most important predictors in the boosted regression tree. As expected, municipality-months with spillover had higher lagged and current environmental risk, as well as high (phenomenologically) estimated primate infection prevalence and high primate species richness. Municipality-months with spillover tended to have vaccine coverage above 75%. While estimated vaccine coverage was included as a measure of human susceptibility, it is likely capturing other patterns in the spatial distribution of spillover; regions known to experience

yellow fever spillover are likely to have high vaccination rates, while those where spillover is rare or nonexistent are likely to have low vaccination rates. Accordingly, estimated vaccine coverage is bimodal, potentially due to a group of lower risk municipalities and a group of higher risk municipalities. The partial dependence plot also displays two plateaus in the marginal effect in the vaccine coverage on model estimates, which roughly correspond to the two vaccine coverage groups. We find that municipality-months with spillover have low monthly precipitation (Fig. 4), which may correspond to settings with increased human activity in the forest, and therefore increased chance of spillover. However, current and lagged fire area, hypothesized indicators of deforestation activity, were not significant predictors of spillover in the boosted regression tree models (Supplementary Materials, Fig. S8).

The recent outbreaks in Brazil in the 2016–2017 and 2017–2018 transmission seasons have been the largest in over 50 years (16). The environmental risk model finds that spillover in the affected states (Minas Gerais, Espirito Santo, Sao Paulo, and Rio de Janeiro) is consistent with the persistent low environmental risk in the area (Fig. 5) and does not predict any elevation in spillover risk during the recent transmission seasons. As in other regions, the model accurately captures the seasonality of spillover risk in this region (Fig. 5), which is distinct from that of other regions (Fig. 3a).

Discussion

Our mechanistic understanding of environmental risk of spillover—which combines reservoir host and sylvatic vector distributions, vector contact with reservoirs and humans, and vector dispersal, survival, infectiousness, and seasonal abundance—predicts yellow fever spillover into humans with high accuracy (AUC = 0.71; Fig. 2). Within each municipality and month, the maximum risk, rather than the mean risk, was the best predictor of spillover occurrence, suggesting that heterogeneity in risk at scales smaller than the municipality is important for determining spillover probability. Rainfall-driven seasonality in the mosquito populations accurately predicted seasonal variation in spillover. While interannual variation in risk was not well-predicted in the environmental risk model based on climate and land cover information alone, including phenomenologically modeled variation in primate yellow fever infection prevalence improved predictions of year-to-year variation in spillover (AUC = 0.79).

Although we hypothesized that low vaccination coverage and high human population density would each increase spillover risk, neither improved model accuracy for predicting spillover in the mechanistic model (Fig. 2). However, we found that vaccine coverage was the second most important predictor of municipality-months with spillover when allowing for a nonlinear, positive relationship between coverage and spillover probability (Fig. 4). By contrast, as expected, vaccine coverage was a significant negative predictor of the number of cases in municipality-months with spillover, consistent with the high numbers of cases in the recent spillover-driven outbreaks in Southeast Brazil in 2016–2018 where prior vaccination rates were low (11). The recent outbreak is also consistent with the ecological processes driving past spillover in this region (Fig. 5). While environmental risk in 2016–2018 was not elevated above historical levels (2001–2015) and spillover had not occurred in in the states of Espirito Santo or Rio de Janeiro during the previous 15 years, it has previously occurred in Minas Gerais and Sao Paulo states in 2001–2003 and 2008–2009. Data from the 2016–2018 outbreak (past December 2016) are not included in the statistical models because consistent monthly municipality-scale spillover data across the country are not available for that period.

The boosted regression tree analysis, which aimed to detect candidate drivers of spillover that might be missing from our mechanistic model, identified vaccine coverage, current and lagged environmental risk, temperature, population density, and precipitation as important

predictors, which together improved upon mechanistic model predictive performance of pathogen spillover (out-of-sample AUC = 0.95). The relative importance of lagged and current environmental risk provides evidence that the mechanistic model captures the potentially nonlinear and interactive relationship between environmental variables that drive spillover in mosquitoes, reservoir hosts, and humans better than the environmental variables alone. One month lagged environmental risk may be more important than current environmental risk for predicting spillover because of a lag between cases and reporting. Additionally, environmental suitability for reservoir and vectors may drive reservoir infection dynamics, causing a lag between conditions suitable for virus amplification in the primate reservoir and vector populations, and spillover into humans.

In a recent paper, Kaul et al. (8) also used a machine learning approach to predict municipality-months with spillover in Brazil and similarly found rainfall and precipitation to be important predictors. However, their model also identified primate richness and fire density as important predictors, while our boosted regression tree analysis ranked municipality average primate richness ninth, municipality maximum primate richness fourteenth, lagged fire area tenth, and current fire area eleventh for variable importance out of fourteen variables. Our covariates add to those used by Kaul et al. (8) by including vaccine coverage and our mechanistic environmental risk estimate (current and lagged), which boosted regression trees found to be three of the four most important predictors. We expect that our mechanistic environmental risk estimates capture much of the variation attributed to other environmental variables in the Kaul et al. model. Despite the differing relative importance of variables for predicting spillover in the two models, they both predict that seasonal patterns vary by regions of Brazil and find Southeast Brazil seasonally suitable for yellow fever spillover.

Given the importance of vaccination campaigns in limiting yellow fever outbreaks, we expected that the number of susceptible (unvaccinated) people would be an important positive predictor of yellow fever spillover occurrence, yet mechanistic population-scaled risk performed worse at predicting spillover than environmental risk alone (Fig. 2). For example, scaling by population size predicts areas of very high risk along the coast of Brazil, where environmental risk is low, but population sizes are high. We predict that vaccination coverage and human density may be more predictive of the number of cases in spillover events (for example, the recent outbreak in Southeast Brazil) than the probability of spillover occurring, given that very low environmental suitability will be amplified in large, unvaccinated populations. We also hypothesize that although vaccine coverage was not predictive of spillover probability, it may be limiting the number of cases in municipality-months with spillover (Supplementary Materials, Table S5), preventing onward transmission, and limiting the potential for urban transmission cycles to develop following spillover.

The substantial improvement in model prediction from environmental to periodic-environmental risk (AUC = 0.71 vs. 0.79) suggests that primate population dynamics, immunity, and infection prevalence may be a key missing component of this mechanistic model. Ongoing surveillance efforts in Brazil are used to detect non-human primate cases of yellow fever as an advanced warning system (69). While this advanced warning system can make a critical difference, the recent outbreaks in Southeast Brazil displayed that in some cases this surveillance may not provide sufficient time to respond to prevent spillover, especially in areas with high populations and low vaccine coverage rates as were found in the Southeast. Incorporating a mechanistic model of non-human primate infection prevalence, driven by local primate surveillance data, could help to indicate when primate cases of yellow fever are likely, to provide additional time for public health officials to respond. This remains a significant and potentially very fruitful gap in our understanding of yellow fever transmission and spillover.

Vector-human contact rates are another important empirical gap in the mechanistic model, which could further refine the relationships between land use, human occupations and behavior, and spillover risk. We approximate human contact rates with sylvatic vectors with percent forest cover, but the relationship is likely much more complex. The surprising decreasing relationship between precipitation and spillover probability in the boosted regression tree (Fig. 4) may be due to the influence of precipitation on human activities in and around forests, and therefore its influence on human-vector contact (36).

Yellow fever is an ancient, historically important human disease that played a central role in the discovery of mosquito transmission of pathogens and the subsequent development of vector control as a public health measure (70). The wealth of existing knowledge about the ecology of yellow fever virus and its sylvatic reservoir hosts and vectors allowed us to synthesize data from 73 published papers to mathematically formalize our ecological understanding of sylvatic transmission and spillover. Although spillover is a stochastic process that is expected to be difficult to predict, the mechanistic model that integrates vector, human host, non-human reservoir, and virus ecology allowed us to predict spillover with surprising accuracy. Historically in the Americas and presently in other regions such as sub-Saharan Africa, yellow fever regularly has entered urban transmission cycles that lead to major human epidemics. The model framework presented here could be extended to include the ecology of different vectors, hosts, and environments, including urban *Aedes aegypti* and more human immune interactions with other flaviviruses, to ask intriguing questions such as: What prevents yellow fever from entering urban transmission cycles in the Americas, where other flavivirus epidemics regularly occur? Why has urban transmission occurred recently in Africa and not in South America? What prevents yellow fever circulation and spillover in Southeast Asia, where sylvatic vectors and non-human primate hosts are present and the climate is suitable? Answers to these questions would further our understanding of the ecology of (re)emerging diseases in different parts of the world. More fundamentally, this work provides clear evidence for the predictive power of mechanistic, ecological models—even for rare events like pathogen spillover—and can provide useful information to enhance public health interventions of zoonotic diseases.

Additional Information

Acknowledgements

Freya Shearer kindly provided data on vaccine coverage estimates. We thank the Defense Advanced Research Projects Agency whose funding provided the opportunity to discuss and develop this project at a workshop on pathogen spillover. We would also like to thank the many previous studies who have made their data available as well as publicly available remote sensing data that made this project possible.

Data Accessibility

All data and code are available on GitHub (https://github.com/marissachilds/YellowFeverSpillover).

Authors' Contributions

MLC and EAM conceived of the project and designed the analyses. MLC, NN, and JC collected the data and performed the analyses. MLC drafted the manuscript. EAM, NN, and JC revised the manuscript and all authors read and approved the final manuscript.

Competing Interests

We have no competing interests.

Funding
MLC was funded by the Lindsay Family E-IPER Fellowship. NN was funded by The Bing Fellowship in Honor of Paul Ehrlich. JC was funded by the Stanford University Biology Summer Undergraduate Research Program. EAM was funded by the National Science Foundation Ecology and Evolution of Infectious Diseases program (DEB-1518681), the Stanford University Woods Institute for the Environment – Environmental Ventures Program, and the Hellman Faculty Fellowship.

References

1. Woolhouse MEJ, Haydon DT, Antia R. Emerging pathogens: The epidemiology and evolution of species jumps. Trends Ecol Evol. 2005;20(5):238–44. https://doi.org/10.1016/j.tree.2005.02.009
2. Jones KE, Patel NG, Levy MA, Storeygard A, Balk D, Gittleman JL, et al. Global trends in emerging infectious diseases. Nature. 2008;451(7181):990–3. https://doi.org/10.1038/nature06536
3. Plowright RK, Parrish CR, McCallum H, Hudson PJ, Ko AI, Graham AL, et al. Pathways to zoonotic spillover. Nat Rev Microbiol [Internet]. 2017 May 30;15(8):502–10. https://doi.org/10.1038/nrmicro.2017.45
4. Plowright RK, Eby P, Hudson PJ, Smith IL, Westcott D, Bryden WL, et al. Ecological dynamics of emerging bat virus spillover. Proc R Soc B Biol Sci [Internet]. 2014;282(1798):20142124–20142124. https://doi.org/10.1098/rspb.2014.2124
5. Lloyd-Smith JO, George D, Pepin KM, Pitzer VE, Pulliam JRC, Dobson AP, et al. Epidemic Dynamics at the Human-Animal Interface. Science (80-) [Internet]. 2009;326(5958):1362–7. https://doi.org/10.1126/science.1177345
6. Hamrick PN, Aldighieri S, Machado G, Leonel DG, Vilca LM, Uriona S, et al. Geographic patterns and environmental factors associated with human yellow fever presence in the Americas. PLoS Negl Trop Dis. 2017;11(9):1–27.
7. Schmidt JP, Park AW, Kramer AM, Han BA, Alexander LW, Drake JM. Spatiotemporal fluctuations and triggers of ebola virus spillover. Emerg Infect Dis. 2017;23(3):415–22. https://doi.org/10.3201/eid2303.160101
8. Kaul RB, Evans M V., Murdock CC, Drake JM. Spatio-temporal spillover risk of yellow fever in Brazil. Parasit Vectors [Internet]. 2018;11(1):488. https://doi.org/10.1186/s13071-018-3063-6
9. Monath TP, Vasconcelos PFC. Yellow fever. J Clin Virol [Internet]. 2015;64:160–73. https://doi.org/10.1016/j.jcv.2014.08.030
10. Paules CI, Fauci AS. Yellow Fever — Once Again on the Radar Screen in the Americas. N Engl J Med [Internet]. 2017;376(15):1397–9. https://doi.org/10.1056/NEJMp1002530
11. Faria NR, Kraemer MUG, Hill SC, Goes de Jesus J, Aguiar RS, Iani FCM, et al. Genomic and epidemiological monitoring of yellow fever virus transmission potential. Science (80-) [Internet]. 2018 Aug 31;361(6405):894–9. https://doi.org/10.1126/science.aat7115
12. Hanley KA, Monath TP, Weaver SC, Rossi SL, Richman RL, Vasilakis N. Fever versus fever: The role of host and vector susceptibility and interspecific competition in shaping the current and future distributions of the sylvatic cycles of dengue virus and yellow fever virus. Infect Genet Evol [Internet]. 2013 Oct;19:292–311. https://doi.org/10.1016/j.meegid.2013.03.008
13. Johansson MA, Vasconcelos PFC, Staples JE. The whole iceberg: Estimating the incidence of yellow fever virus infection from the number of severe cases. Trans R Soc Trop Med Hyg. 2014;108(8):482–7. https://doi.org/10.1093/trstmh/tru092
14. Valderrama A, Díaz Y, López-Vergès S. Interaction of Flavivirus with their mosquito vectors and their impact on the human health in the Americas. Biochem Biophys Res Commun. 2017;492:541–7. https://doi.org/10.1016/j.bbrc.2017.05.050
15. de Souza RP, Foster PG, Sallum MAM, Coimbra TLM, Maeda AY, Silveira VR, et al. Detection of a new yellow fever virus lineage within the South American genotype I in Brazil. J Med Virol [Internet]. 2010 Jan;82(1):175–85. https://doi.org/10.1002/jmv.21606
16. Pan American Health Organization / World Health Organization. Epidemiological Update: Yellow Fever (7 December 2018) [Internet]. 2018. Retrieved from

https://www.paho.org/hq/dmdocuments/2017/2017-feb-16-phe-epi-update-yellow-fever.pdf
17. Shearer FM, Moyes CL, Pigott DM, Brady OJ, Marinho F, Deshpande A, et al. Global yellow fever vaccination coverage from 1970 to 2016: An adjusted retrospective analysis. Lancet Infect Dis. 2017;3099(17):1–9. https://doi.org/10.1016/S1473-3099(17)30419-X
18. Vasconcelos PF da C. Yellow fever in Brazil: thoughts and hypotheses on the emergence in previously free areas. Rev Saude Publica [Internet]. 2010;44(6):1144–9. https://doi.org/10.1590/S0034-89102010005000046
19. Gorelick N, Hancher M, Dixon M, Ilyushchenko S, Thau D, Moore R. Google Earth Engine: Planetary-scale geospatial analysis for everyone. Remote Sens Environ [Internet]. 2017; https://doi.org/10.1016/j.rse.2017.06.031
20. IUCN. The IUCN Red List of Threatened Species. Version 2018-2. 2018.
21. Center for International Earth Science Information Network - CIESIN - Columbia University. Gridded Population of the World, Version 4 (GPWv4): Population Count Adjusted to Match 2015 Revision of UN WPP Country Totals. 2016. https://doi.org/10.7927/H4SF2T42
22. R Core Team. R: A Language and Environment for Statistical Computing [Internet]. Vienna, Austria; 2018. Retrieved from https://www.r-project.org/
23. Wickham H. The Split-Apply-Combine Strategy for Data Analysis. J Stat Softw [Internet]. 2011;40(1):1–29. Retrieved from http://www.jstatsoft.org/v40/i01/
24. Wickham H, François R, Henry L, Müller K. dplyr: A Grammar of Data Manipulation [Internet]. 2018. Retrieved from https://cran.r-project.org/package=dplyr
25. Bache SM, Wickham H. magrittr: A Forward-Pipe Operator for R [Internet]. 2014. Retrieved from https://cran.r-project.org/package=magrittr
26. Bivand R, Keitt T, Rowlingson B. rgdal: Bindings for the "Geospatial" Data Abstraction Library [Internet]. 2018. Retrieved from https://cran.r-project.org/package=rgdal
27. Wickham H. stringr: Simple, Consistent Wrappers for Common String Operations [Internet]. 2018. Retrieved from https://cran.r-project.org/package=stringr
28. Hijmans RJ. raster: Geographic Data Analysis and Modeling [Internet]. 2018. Retrieved from https://cran.r-project.org/package=raster
29. Wickham H. ggplot2: Elegant Graphics for Data Analysis [Internet]. Springer-Verlag New York; 2016. Retrieved from http://ggplot2.org
30. Borchers HW. pracma: Practical Numerical Math Functions [Internet]. 2018. Retrieved from https://cran.r-project.org/package=pracma
31. Bivand R, Rundel C. rgeos: Interface to Geometry Engine - Open Source ('GEOS') [Internet]. 2018. Retrieved from https://cran.r-project.org/package=rgeos
32. Phillips SJ, Anderson RP, Schapire RE. Maximum entropy modeling of species geographic distributions. Ecol Modell [Internet]. 2006 Jan;190(3–4):231–59. https://doi.org/10.1016/j.ecolmodel.2005.03.026
33. Elith J, Phillips SJ, Hastie T, Dudík M, Chee YE, Yates CJ. A statistical explanation of MaxEnt for ecologists. Divers Distrib. 2011;17(1):43–57. https://doi.org/10.1111/j.1472-4642.2010.00725.x
34. Phillips S. maxnet: Fitting "Maxent" Species Distribution Models with "glmnet" [Internet]. 2017. Retrieved from https://cran.r-project.org/package=maxnet
35. Fox SJ, Bellan SE, Perkins TA, Johansson MA, Meyers LA. Downgrading disease transmission risk estimates using terminal importations. bioRxiv [Internet]. 2018; https://doi.org/10.1101/265942
36. Kumm HW. Seasonal variations in rainfall: Prevalence of Haemagogus and incidence of

jungle yellow fever in Brazil and Colombia. Trans R Soc Trop Med Hyg. 1950;43(6):673–82. https://doi.org/10.1016/0035-9203(50)90009-5
37. Causey OR, Dos Santos G V. Diurnal Mosquitoes in an Area of Small Residual Forests in Brazil1. Ann Entomol Soc Am [Internet]. 1949 Dec 1;42(4):471–82. https://doi.org/10.1093/aesa/42.4.471
38. Chadee DD. Seasonal abundance and diel landing periodicity of Sabethes chloropterus (Diptera: Culicidae) in Trinidad, West Indies. J Med Entomol. 1990;27(6):1041–4. https://doi.org/10.1093/jmedent/27.6.1041
39. Chadee DD, Tikasingh ES, Ganesh R. Seasonality, biting cycle and parity of the yellow fever vector mosquito Haemagogus janthinomys in Trinidad. Med Vet Entomol. 1992;6(2):143–8. https://doi.org/10.1111/j.1365-2915.1992.tb00592.x
40. Chadee DD, Ganesh R, Hingwan JO, Tikasingh ES. Seasonal abundance, biting cycle and parity of the mosquito Haemagogus leucocelaenus in Trinidad, West Indies. Med Vet Entomol [Internet]. 1995 Oct;9(4):372–6. https://doi.org/10.1111/j.1365-2915.1995.tb00006.x
41. Medeiros AS, Marcondes CB, De Azevedo PRM, Jerônimo SMB, e Silva VPM, Ximenes MDFFDM. Seasonal variation of potential flavivirus vectors in an urban biological reserve in northeastern Brazil. J Med Entomol [Internet]. 2009;46(6):1450–7. https://doi.org/10.1603/033.046.0630
42. Tubaki RM, Menezes RMT De, Vesgueiro FT, Cardoso RP. Observations on Haemagogus janthinomys Dyar (Diptera: Culicidae) and other mosquito populations within tree holes in a gallery forest in the northwestern region of Sao Paulo state, Brazil. Neotrop Entomol. 2010;39(4):664–70. https://doi.org/Doi 10.1590/S1519-566x2010000400030
43. Bates M. The Development and Longevity of Haemagogus Mosquitoes under Laboratory Conditions1. Ann Entomol Soc Am [Internet]. 1947 Mar 1;40(1):1–12. https://doi.org/10.1093/aesa/40.1.1
44. Galindo P. Bionomics of Sabethes Chloropterus Humboldt, a Vector of Sylvan Yellow Fever in Middle America 1. Am J Trop Med Hyg [Internet]. 1958 Jul 1;7(4):429–40. https://doi.org/10.4269/ajtmh.1958.7.429
45. Dégallier N, SÁ Filho GC, Monteiro HAO, Castro FC, Vaz Da Silva O, Brandão RCF, et al. Release–Recapture Experiments with Canopy Mosquitoes in the Genera Haemagogus and Sabeihes (Diptera: Culicidae) in Brazilian Amazonia. J Med Entomol [Internet]. 1998 Nov 1;35(6):931–6. https://doi.org/10.1093/jmedent/35.6.931
46. Team SD. RStan: the R interface to Stan [Internet]. 2018. Retrieved from http://mc-stan.org/
47. Clements AN, Paterson GD. The Analysis of Mortality and Survival Rates in Wild Populations of Mosquitoes. J Appl Ecol [Internet]. 1981 Aug;18(2):373. https://doi.org/10.2307/2402401
48. Tesla B, Demakovsky LR, Mordecai EA, Ryan SJ, Bonds MH, Ngonghala CN, et al. Temperature drives Zika virus transmission: Evidence from empirical and mathematical models. Proc R Soc B Biol Sci. 2018;285(1884). https://doi.org/10.1098/rspb.2018.0795
49. Mordecai EA, Cohen JM, Evans M V, Gudapati P, Johnson LR, Lippi CA, et al. Detecting the impact of temperature on transmission of Zika, dengue, and chikungunya using mechanistic models. Althouse B, editor. PLoS Negl Trop Dis [Internet]. 2017 Apr 27;11(4):e0005568. https://doi.org/10.1371/journal.pntd.0005568
50. Johansson MA, Arana-Vizcarrondo N, Biggerstaff BJ, Staples JE. Incubation periods of yellow fever virus. Am J Trop Med Hyg. 2010;83(1):183–8.

https://doi.org/10.4269/ajtmh.2010.09-0782
51. Chan M, Johansson MA. The Incubation Periods of Dengue Viruses. PLoS One. 2012;7(11):1–7. https://doi.org/10.1371/journal.pone.0050972
52. Kumm HW, Waddell MB. Haemagogus Capricornii Lutz as a Laboratory Vector of Yellow Fever 1. Am J Trop Med Hyg [Internet]. 1948 Mar 1;s1-28(2):247–52. https://doi.org/10.4269/ajtmh.1948.s1-28.247
53. Roca-García M, Bates M. The Development of the Virus of Yellow Fever in Haemagogus Mosquitoes. Am J Trop Med Hyg [Internet]. 1946 Sep 1;s1-26(5):585–605. https://doi.org/10.4269/ajtmh.1946.s1-26.585
54. ANDERSON CR, OSORNO-MESA E. The laboratory transmission of yellow fever virus by Haemagogus splendens. Am J Trop Med Hyg [Internet]. 1946 Sep;26(5):613–8. Retrieved from http://www.ncbi.nlm.nih.gov/pubmed/21003269
55. Waddell MB, Taylor RM. Studies on Cyclic Passage of Yellow Fever Virus in South American Mammals and Mosquitoes: Marmosets (Callithrix aurita) and Cebus Monkeys (Cebus versutus) in Combination with Aedes aegypti and Haemagogus equinus. Am J Trop Med Hyg [Internet]. 1945 May 1;s1-25(3):225–30. https://doi.org/10.4269/ajtmh.1945.s1-25.225
56. Roca-Garcia M, Bates M. Laboratory Studies of the Saimiri-Haemagogus Cycle of Jungle Yellow Fever. Am J Trop Med Hyg [Internet]. 1945 May 1;s1-25(3):203–16. https://doi.org/10.4269/ajtmh.1945.s1-25.203
57. Galindo P, Trapido H, de Rodaniche E. Experimental Transmission of Yellow Fever by Central American Species of Haemagogus and Sabethes Chloropterus. Am J Trop Med Hyg [Internet]. 1956 Nov 1;5(6):1022–31. https://doi.org/10.4269/ajtmh.1956.5.1022
58. WADDELL MB. Comparative efficacy of certain South American Aëdes and Haemagogus mosquitoes as laboratory vectors of yellow fever. Am J Trop Med Hyg [Internet]. 1949 Jul;29(4):567–75. Retrieved from http://www.ncbi.nlm.nih.gov/pubmed/18153054
59. Waddell MB, Taylor RM. Studies on the Cyclic Passage of Yellow Fever Virus in South American Mammals and MosquitoesI III. Further Observations on Haemagogus equinus as a vector of the virus. Am J Trop Med Hyg [Internet]. 1947 Jul 1;s1-27(4):471–6. https://doi.org/10.4269/ajtmh.1947.s1-27.471
60. Estep LK, Burkett-Cadena ND, Hill GE, Unnasch RS, Unnasch TR. Estimation of Dispersal Distances of Culex erraticus in a Focus of Eastern Equine Encephalitis Virus in the Southeastern United States. J Med Entomol [Internet]. 2010;47(6):977–86. https://doi.org/10.1603/ME10056
61. CAUSEY OR, KUMM HW. Dispersion of forest mosquitoes in Brazil; preliminary studies. Am J Trop Med Hyg [Internet]. 1948 May;28(3):469–80. Retrieved from http://www.ncbi.nlm.nih.gov/pubmed/18859835
62. Camara FP, Gomes ALBB, Carvalho LMF de, Castello LGV. Dynamic behavior of sylvatic yellow fever in Brazil (1954-2008). Rev Soc Bras Med Trop [Internet]. 2011 Jun;44(3):297–9. https://doi.org/10.1590/S0037-86822011005000024
63. Elith J, Leathwick JR, Hastie T. A working guide to boosted regression trees. J Anim Ecol. 2008;77(4):802–13. https://doi.org/10.1111/j.1365-2656.2008.01390.x
64. Han BA, Schmidt JP, Alexander LW, Bowden SE, Hayman DTS, Drake JM. Undiscovered Bat Hosts of Filoviruses. PLoS Negl Trop Dis. 2016;10(7):1–10. https://doi.org/10.1371/journal.pntd.0004815
65. Millones M, Rogan J, II BL, Parmentier B, Harris R, Griffith D. Fire Data as Proxy for Anthropogenic Landscape Change in the Yucatán. Land [Internet]. 2017;6(3):61.

https://doi.org/10.3390/land6030061
66. Greenwell B, Boehmke B, Cunningham J, Developers GBM. gbm: Generalized Boosted Regression Models [Internet]. 2018. Retrieved from https://cran.r-project.org/package=gbm
67. Hijmans RJ, Phillips S, Leathwick J, Elith J. dismo: Species Distribution Modeling [Internet]. 2017. Retrieved from https://cran.r-project.org/package=dismo
68. Greenwell BM. pdp: An R Package for Constructing Partial Dependence Plots. R J [Internet]. 2017;9(1):421–36. Retrieved from https://journal.r-project.org/archive/2017/RJ-2017-016/index.html
69. Almeida MAB, da Cardoso JC, dos Santos E, da Fonseca DF, Cruz LL, Faraco FJC, et al. Surveillance for Yellow Fever Virus in Non-Human Primates in Southern Brazil, 2001-2011: A Tool for Prioritizing Human Populations for Vaccination. PLoS Negl Trop Dis. 2014;8(3). https://doi.org/10.1371/journal.pntd.0002741
70. Gorgas WC. Sanitation in Panama. Appleton; 1915.

Tables

Table 1

Variable	Definition	Model
$\beta_h(\vec{x},t)$	Proportion of mosquito bites from sylvatic vectors on humans at location $\vec{x}$ at time t	Approximated as $1-f(\vec{x},t)$ in locations with non-zero human population density, where $f(\vec{x},t)$ is the percent forest cover at location $\vec{x}$ at time t
$\beta_p(\vec{x},t)$	Proportion of mosquito bites from sylvatic vectors on non-human primates at location $\vec{x}$ at time t	Approximated as $f(\vec{x},t)$ in locations within at least one non-human primate range, where $f(\vec{x},t)$ is the percent forest cover at location $\vec{x}$ at time t
$\rho_v(\vec{x},t)$	Sylvatic vector density at location $\vec{x}$ at time t	Approximated as location maximum mosquito density multiplied by relative seasonal abundance, where maximum mosquito density is determined by a species distribution model and seasonal abundance is modeled from field capture data (see Methods: Mechanism models)
$EIP(T(\vec{x},t),\Delta t)$	Probability a mosquito that took an infectious blood meal becomes infectious with yellow fever virus given a temperature $T(\vec{x},t)$ and Δt days elapsing	See Methods: Mechanistic models
$s(T(\vec{x},t),\Delta t)$	Probability that a mosquito survives Δt days given a temperature $T(\vec{x},t)$	See Methods: Mechanistic models
$d(\lVert\vec{x}-\vec{y}\rVert)$	Probability that a mosquito disperses from $\vec{x}$ to $\vec{y}$	See Methods: Mechanistic models
$b(\vec{x},t)$	Biting rate of sylvatic vectors at location $\vec{x}$ at time t	Assumed constant given limited information on determinants of vector biting rates
$\kappa(\vec{x},t)$	Infection prevalence in nonhuman primate reservoir at location $\vec{x}$ at time t	For environmental risk metric, assumed constant given limited information of nonhuman primate infection prevalence. For periodic-environmental risk metric, used periodic curve fit to yearly case data (see Methods: Phenomenological primate dynamics).

Figure and Table Captions

Table 1. Spillover model variables and definitions.

Figure 1. Spillover model components and observed spillover in Brazil (2001–2016). Spatial distributions of primate reservoir species (a), vector species (b), reservoir-vector contact (c), human-vector contact (f), and human susceptibility as estimated by one minus vaccine coverage (i). Mechanistic mosquito models dependent on distance for mosquito dispersal (d), temperature for mosquito survival (e) and mosquito infectiousness (g), and rainfall for mosquito abundance (h). All mechanistic model components (a–i) are derived from empirical data. Observed data on number of municipality-months with spillover into humans by year (j) and municipality (k) are used to test the mechanistic models.

Figure 2. Municipality maximum periodic-environmental risk best predicts spillover. Each point is the calculated area under the curve (AUC) from spillover predicted by modeled risk, where higher AUC represents a model better able to distinguish between spillover and non-spillover observations. The risk models (from left to right on the x-axis) are: environmental risk, periodic-environmental risk, immunological-environmental risk, and population-scaled risk. Municipality-wide maxima (red dashed lines and circles) and means (blue dotted lines and triangles) are shown for each metric.

Figure 3. Modeled environmental risk captures seasonal variation and periodic-environmental risk captures interannual variation in spillover. Each colored line is the seasonal average of modeled maximum environmental risk in a municipality (a) and the yearly average of modeled maximum periodic-environmental risk in a municipality (b). Black lines are the regional average over the municipal curves. Points represent the total number of municipality-months with spillover in that region per month (a) or per year (b). Correlations between regional average environmental risk and regional number of municipality-months with spillover shown in parentheses for regions where spillover has occurred (all except the Northeast). Regions of Brazil are shown with corresponding colors (c); hatching indicates the states that experienced spillover during the large outbreak in 2016–2018.

Figure 4. Partial dependence plots of top six predictors of spillover in a municipality-month from boosted regression tree analysis. Plots are listed in order of predictive importance with relative influence (%) listed. Histograms show the distribution of observed municipality-months at each covariate value (left axis) and solid lines show the marginal effects of covariate on model prediction (right axis). Marginal effects highlight the characteristics of municipality-months that experienced spillover in Brazil 2001–2016.

Figure 5: Mechanistic model predicts consistent low, seasonal risk in Southeast region of Brazil (2001–2018). Grey lines are municipality estimates of maximum environmental risk and the black line is the environmental risk averaged over all municipalities in the state. Red dots are municipality-months with spillover (2001–2016), showing both the date of the spillover and the predicted environmental risk for the municipality during the month of spillover. Human spillover data span January 2001 to December 2016 and the large outbreaks in the Southeast began in December 2016 (dashed blue line).

Figures

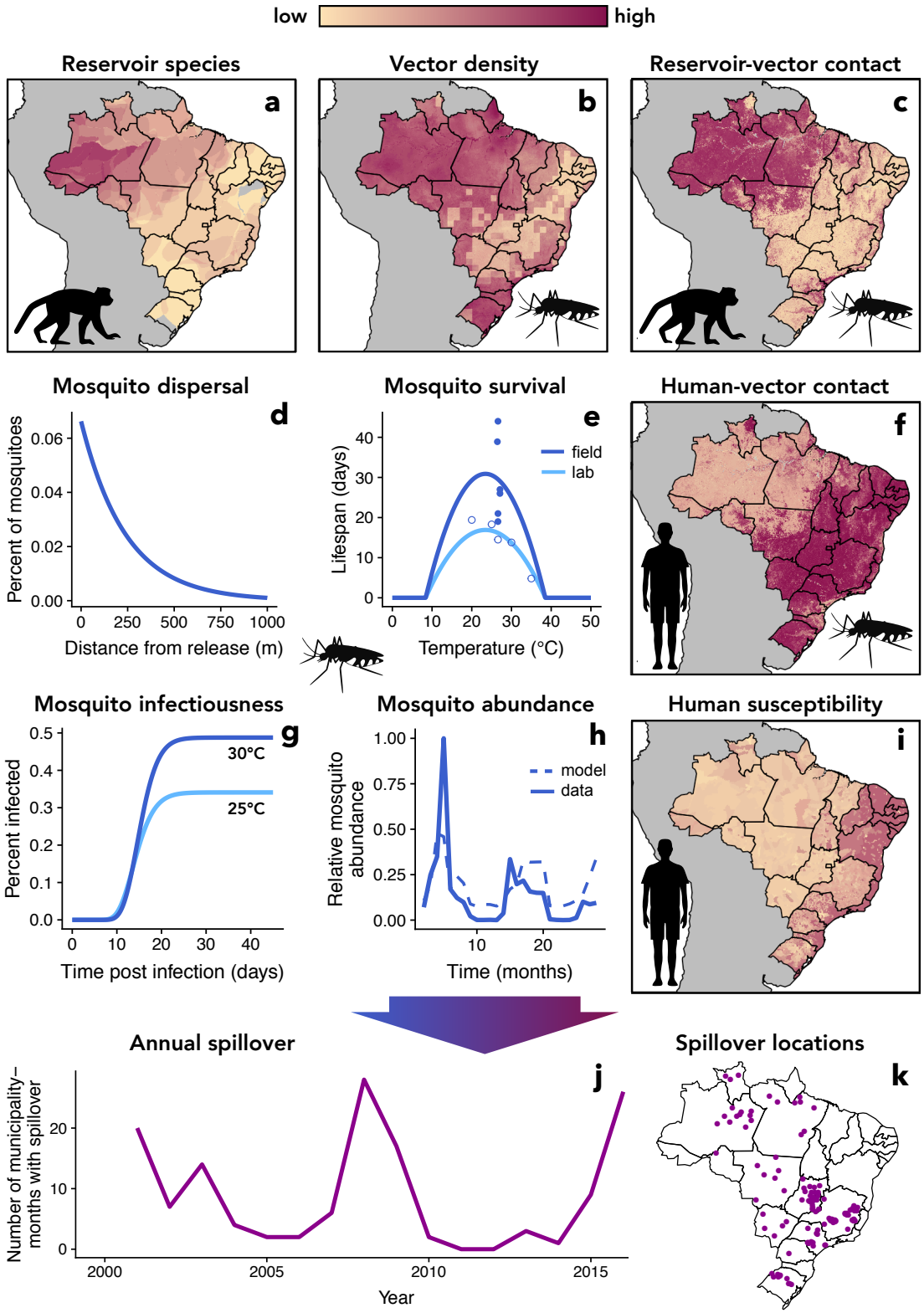

Figure 1

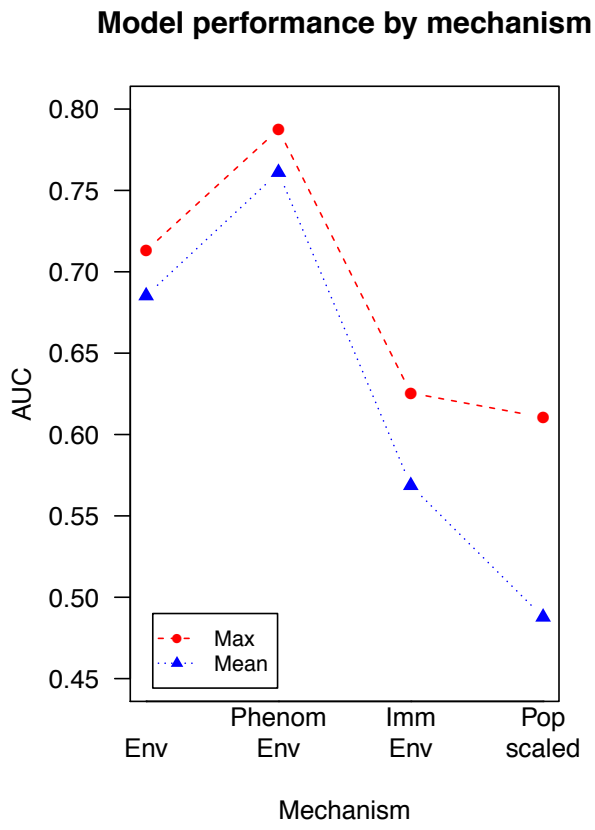
Model performance by mechanism
AUC
0.80
0.75
0.70
0.65
0.60
0.55
0.50
0.45
Max
Mean
Env
Phenom Env
Imm Env
Pop scaled
Mechanism

Figure 2

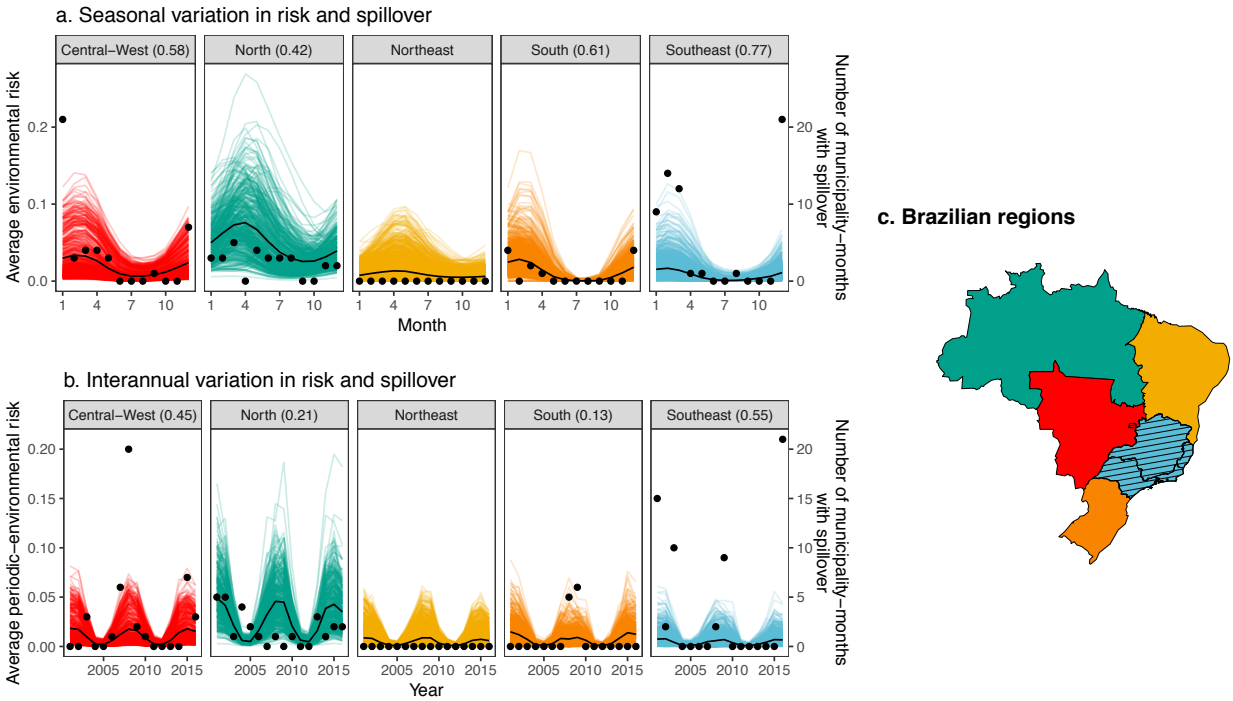
a. Seasonal variation in risk and spillover
Central–West (0.58)
North (0.42)
Northeast
South (0.61)
Southeast (0.77)
Average environmental risk
Number of municipality–months with spillover
Month
b. Interannual variation in risk and spillover
Central–West (0.45)
North (0.21)
Northeast
South (0.13)
Southeast (0.55)
Average periodic–environmental risk
Year
c. Brazilian regions

Figure 3

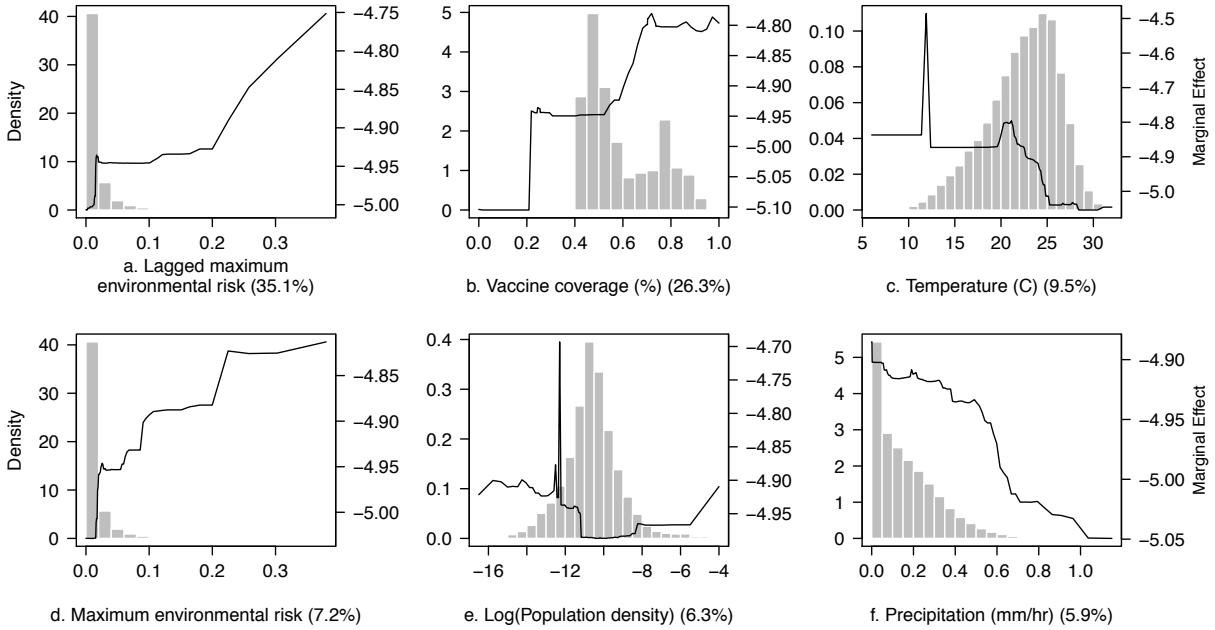
Density
Marginal Effect
a. Lagged maximum environmental risk (35.1%)
b. Vaccine coverage (%) (26.3%)
c. Temperature (C) (9.5%)
d. Maximum environmental risk (7.2%)
e. Log(Population density) (6.3%)
f. Precipitation (mm/hr) (5.9%)

Figure 4

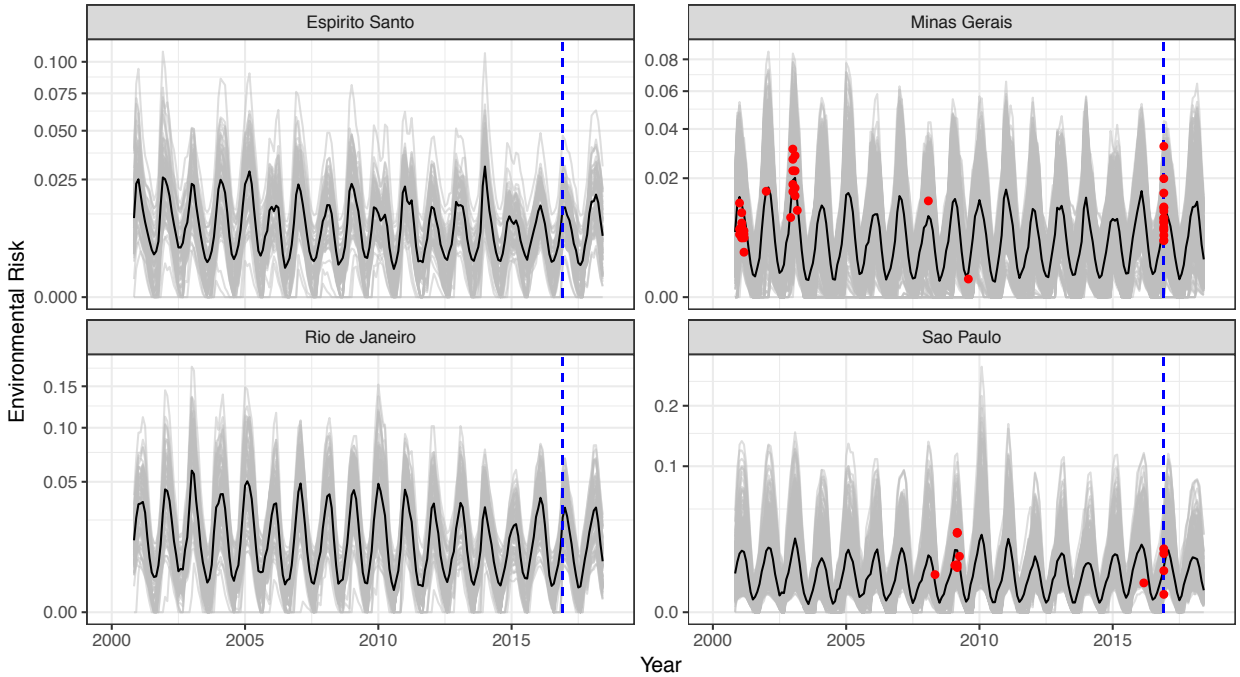
Espirito Santo
Minas Gerais
Rio de Janeiro
Sao Paulo
Environmental Risk
Year
0.100
0.075
0.050
0.025
0.000
0.08
0.06
0.04
0.02
0.00
0.15
0.10
0.05
0.00
0.2
0.1
0.0
2000
2005
2010
2015

Figure 5